

Thermodynamic Limit for Excitonic Light-Emitting Diodes

Noel C. Giebink^{1,2,*} and Stephen R. Forrest¹

¹*Department of Electrical Engineering and Computer Science, and Physics, University of Michigan, Ann Arbor, Michigan 48109, USA*

²*Department of Electrical Engineering, The Pennsylvania State University, University Park, Pennsylvania 16802, USA*

 (Received 8 January 2023; revised 28 February 2023; accepted 7 June 2023; published 29 June 2023)

We derive the thermodynamic limit for organic light-emitting diodes (OLEDs), and show that strong exciton binding in these devices requires a higher voltage to achieve the same luminance as a comparable inorganic LED. The OLED overpotential, which does not reduce the power conversion efficiency, is minimized by having a small exciton binding energy, a long exciton lifetime, and a large Langevin coefficient for electron-hole recombination. Based on these results, it seems likely that the best phosphorescent and thermally activated delayed fluorescence OLEDs reported to date approach their thermodynamic limit. The framework developed here is broadly applicable to other excitonic materials, and should therefore help guide the development of low voltage LEDs for display and solid-state lighting applications.

DOI: [10.1103/PhysRevLett.130.267002](https://doi.org/10.1103/PhysRevLett.130.267002)

Organic light-emitting diodes (OLEDs) have matured over the past thirty years to the point that they are now the basis for most mobile displays sold worldwide. State-of-the-art OLEDs routinely operate with 100% internal quantum efficiency (where every injected electron produces a photon) at voltages close to the emitted photon energy. [1–8] It is therefore important to understand the thermodynamic limit of these devices, which has so far been assumed [2] to be equal to that of inorganic LEDs as given by the generalized Planck equation assuming equilibrium between the radiation field and free electrons and holes [4,5,9]. In organic semiconductors, however, strongly bound Frenkel excitons are the primary photoexcitation, [10] and thus the radiation field in this case is in equilibrium with excitons, not free electrons and holes. Since the chemical potential of excitons is in general different than the electron-hole quasi-Fermi level splitting (i.e., the difference of the electron and hole electrochemical potentials), the thermodynamic limit for OLEDs is expected to differ from that of inorganic LEDs, similar to the case of photovoltaic cells [11,12].

In this Letter, we show that the drive voltage of an ideal OLED depends on the dissociation efficiency of its emissive excitons. When exciton dissociation is not efficient, the voltage required for an OLED to achieve the same luminance as a corresponding inorganic LED with all other factors being equal, is higher by $\Delta V_{\text{op}} = (k_B T/q) \ln(1 + k_r e^{E_b/k_B T} / \gamma N_{\text{mol}})$, where E_b is the exciton binding energy, k_r is the exciton radiative rate, γ is the Langevin recombination coefficient, $k_B T$ is the thermal energy, q is the electronic charge, and N_{mol} is the molecular density of the organic semiconductor. Energetic disorder does not significantly alter this overpotential. Surveying the literature, it seems likely that the best phosphorescent and thermally-activated delayed fluorescence (TADF) OLEDs reported to date approach their thermodynamic limit.

In the absence of excitonic effects, the thermodynamic limit for an inorganic LED is determined by the generalized Planck equation [9,13]:

$$\Phi_L = \int_0^\infty dE_{\text{ph}} \int_0^{\pi/2} \left(\frac{2}{h^3 c^2} \right) \frac{E_{\text{ph}}^2 A(E_{\text{ph}}, \theta)}{\exp[(E_{\text{ph}} - \mu_{\text{eh}})/k_B T] - 1} \times 2\pi \times \sin(\theta) \cos \theta d\theta, \quad (1)$$

where Φ_L is the luminescent photon flux emitted from the LED surface, h is Planck's constant, c is the speed of light, and $A(E_{\text{ph}}, \theta)$ is the absorbance of the LED at polar angle, θ , and photon energy, E_{ph} . Equation (1) assumes equilibrium between the radiation field and the gas of free electrons and holes in the semiconductor characterized by their electrochemical potential difference, μ_{eh} . In an ideal device with no series resistance, $\mu_{\text{eh}} = qV$. We note that $A(E_{\text{ph}}, \theta)$ also nominally depends on μ_{eh} (accounting for transparency that occurs upon population inversion); however, this dependence is negligible in the low injection regime of practical interest for LED operation.

Equation (1) applies to organic semiconductors as well (it is closely related to the Kennard-Stepanov relation for molecular luminescence [14–16]). In this case, however, light absorption and emission is mediated by excitons, and thus the relevant chemical potential is that of the exciton population, μ_x . As previously discussed for organic photovoltaics [11], the exciton and free carrier chemical potentials are related via the exciton binding energy and the entropy produced in the exciton dissociation process (ΔS_{diss}):

$$\mu_x = \mu_{\text{eh}} - E_b + T \Delta S_{\text{diss}}. \quad (2)$$

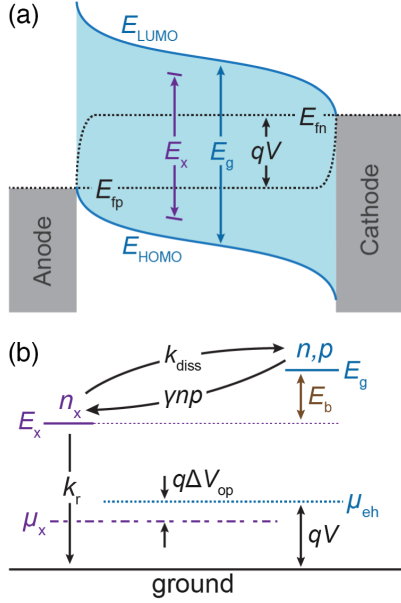


FIG. 1. (a) Band diagram of a canonical OLED characterized by Ohmic bipolar injection and complete electron-hole recombination in an emissive layer. The optical gap set by the exciton energy (E_x) is smaller than the electronic transport gap for free carriers (E_g), defined by the difference between the highest occupied and lowest unoccupied molecular orbital energies (E_{HOMO} and E_{LUMO} , respectively). (b) Kinetic relationship that defines the exciton (n_x) and free carrier (n, p) populations based on the rates of bimolecular recombination (γnp), exciton dissociation (k_{diss}), and radiative recombination (k_r). In general, the exciton and free carrier populations have different chemical potentials (μ_x and μ_{eh} , respectively), which defines the overpotential, ΔV_{op} , required for the OLED to achieve the same luminance as an inorganic LED (where the exciton binding energy, $E_b = 0$) with the same emission energy.

This relationship can be evaluated by considering the rates of bimolecular recombination (γnp), exciton radiative decay (k_r ; the nonradiative decay rate is zero in an ideal OLED) and dissociation (k_{diss}) that determine the exciton density, n_x , according to Fig. 1. Although exciton dissociation is not strictly a first order process, this rate-based approach popularized by Braun [17,18] nevertheless gives the exact Onsager dissociation yield at low electric field [19] and is widely used to describe experimental data in the literature [20,21].

The generalized OLED structure shown in Fig. 1(a) captures the essence of injection and electron-hole recombination in the emissive layer of an actual double heterostructure device without the need to make extraneous assumptions about injection barriers and heterojunction offsets; further discussion is provided in the Supplemental Material [22]. At steady state, the balance of rates for exciton formation and decay in Fig. 1(b) yield the exciton density, $n_x = \gamma np / (k_r + k_{\text{diss}})$. Assuming that Frenkel excitons are localized on individual molecules, and that

each molecule can host only one exciton, n_x is related to μ_x via the Fermi-Dirac occupation function [35]:

$$n_x = \frac{N_{\text{mol}}}{1 + \exp[(E_x - \mu_x)/k_B T]} \approx N_{\text{mol}} \exp[(\mu_x - E_x)/k_B T], \quad (3)$$

where the right-hand equality invokes the Boltzmann approximation when $n_x \ll N_{\text{mol}}$ (i.e., low injection). Under similarly low electron and hole injection, and assuming that each molecule can be occupied by one electron or hole (double occupancy, i.e., a bipolaron, is discouraged owing to the high on-site Coulomb repulsion), the law of mass action gives

$$np \approx N_{\text{mol}}^2 \exp[(\mu_{\text{eh}} - E_g)/k_B T], \quad (4)$$

where E_g denotes the transport gap of the organic semiconductor [Fig. 1(a)]. Substituting Eq. (3) and Eq. (4) into the steady-state relationship between n_x and np , and using $E_g - E_x = E_b$, the exciton chemical potential is therefore

$$\mu_x = \mu_{\text{eh}} - E_b + k_B T \ln \left(\frac{\gamma N_{\text{mol}}}{k_r + k_{\text{diss}}} \right). \quad (5)$$

Equation (5) indicates that an ideal OLED with the same emission energy as an inorganic LED [i.e., the excitonic optical gap, $E_{g,\text{opt}}$, of the OLED equals the band gap, E_g , of the inorganic LED as depicted in Fig. 2(a)] requires an overpotential of $\Delta V_{\text{op}} = E_b/q - (k_B T/q) \ln[\gamma N_{\text{mol}}/(k_r + k_{\text{diss}})]$ to achieve the same luminance via Eq. (1). Although Eq. (5) can be written in terms of the net exciton lifetime, $\tau = (k_r + k_{\text{diss}})^{-1}$, this is deceptive since k_{diss} depends on E_b according to $k_{\text{diss}} = \gamma N_{\text{mol}} \exp(-E_b/k_B T)$ [17,18]. Thus, it is evident that $\mu_x = \mu_{\text{eh}}$ when dissociation is efficient ($k_{\text{diss}} \gg k_r$, which is the limit of an inorganic semiconductor), and that the OLED overpotential is more transparently given by

$$\Delta V_{\text{op}} = \frac{k_B T}{q} \ln \left(1 + \frac{k_r e^{E_b/k_B T}}{\gamma N_{\text{mol}}} \right). \quad (6)$$

The overpotential is, therefore, minimized by having long-lived excitons with a small binding energy and a high Langevin recombination coefficient, which in turn implies high electron and hole mobilities since γ is proportional to their sum [10].

The origin of the overpotential is understood by recognizing that an OLED with the same emission energy as an LED effectively has a larger energy gap from an electrical standpoint (i.e., the gap between the highest occupied and lowest unoccupied molecular orbital transport levels in an organic semiconductor is larger than the excitonic optical gap, $E_g > E_{g,\text{opt}}$). Thus, a given quasi-Fermi level splitting yields a smaller np product and, consequently, a lower

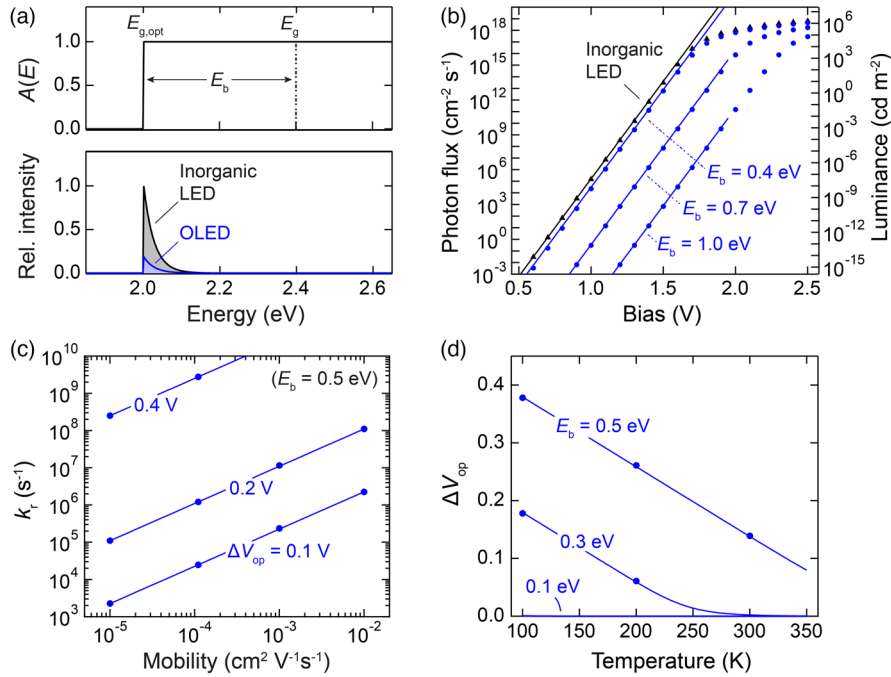


FIG. 2. (a) Absorbance (top) and relative electroluminescence intensity (bottom) for an ideal Lambertian OLED and inorganic LED with the same optical gap. The exciton binding energy of the former is $E_b = 0.4$ eV whereas $E_b = 0$ for the latter. (b) Output photon flux and corresponding luminance of the two devices for varying values of the exciton binding energy assuming $k_r = 1 \mu\text{s}^{-1}$, $N_{\text{mol}} = 10^{21} \text{cm}^{-3}$, and equal electron and hole mobilities, $\mu_n = \mu_p = 10^{-3} \text{cm}^2 \text{V}^{-1} \text{s}^{-1}$, for the OLED. Together with the relative dielectric constant of the organic semiconductor, $\epsilon_r = 3$, and the permittivity of free space, ϵ_0 , these parameters define the Langevin coefficient, $\gamma = q(\mu_n + \mu_p)/(\epsilon_r \epsilon_0)$. The analytical expressions from the text (solid lines) agree well with numerical drift-diffusion simulations (solid circles) carried out using SETFOS. (c) Lines of constant overpotential for varying radiative rate and mobility in the organic semiconductor, assuming $\mu_n = \mu_p$. (d) Temperature dependence of the overpotential for different exciton binding energies, neglecting the temperature dependence of the mobility.

recombination rate. To the extent that excitons live long enough to dissociate, they recycle back into free carriers, thereby helping to sustain a larger quasi-Fermi level splitting, which reduces the required overpotential. Another way of understanding this (which is explicitly evident from the ideal OLED current-voltage relationship derived in the Supplemental Material [22]) is to recognize that an OLED requires more bimolecular recombination events to emit the same number of photons than an inorganic LED with the same band gap since the probability that any given electron-hole recombination event produces a photon in the former [i.e., the radiative yield of the resulting exciton, $k_r/(k_r + k_{\text{diss}})$] is less than for the latter (100%). Note that if equilibrium between excitons and free carriers does not exist due to negligible dissociation, then the overpotential simply equals the exciton binding energy.

Figure 2(a) shows an example for an ideal OLED and inorganic LED with the same 2 eV optical gap. Both devices have the same absorbance and emission spectra; however, the electroluminescence (EL) intensity of the OLED is lower at a given bias owing to its 0.4 eV exciton binding energy. This difference in EL intensity is summarized in Fig. 2(b) for

different values of E_b , and is in agreement with full drift-diffusion simulations that include spatial variation in the free carrier and exciton densities as well as the electric field dependence of the Onsager-Braun dissociation rate [17] (see the Supplemental Material [22] for details). Assuming typical parameters for a phosphorescent OLED, where $E_{g,opt}$ is assumed equal to the triplet exciton energy, the overpotential at room temperature is ~ 0.6 V for $E_b = 1$ eV, and becomes negligible when $E_b \leq 0.3$ eV. Figure 2(c) shows how ΔV_{op} depends on radiative rate and charge carrier mobility (which controls the Langevin coefficient), highlighting the advantage of OLEDs with long-lived phosphorescent or TADF emitters. Finally, the overpotential increases with decreasing temperature in Fig. 2(d) if the mobility is assumed to be constant, and would increase even more if the mobility decreases with temperature as typically occurs in organic semiconductors.

We emphasize that this overpotential does not reduce the OLED power conversion (i.e., wall plug) efficiency; it simply reduces the brightness at a given voltage. Since all recombination is radiative in an ideal device, the current is correspondingly reduced by the overpotential and the power efficiency remains $\eta_p \approx E_{g,opt}/(qV)$, just as for an

inorganic LED. Note that $\eta_p > 1$ for most of the voltage range considered in Fig. 2(b), which corresponds to the electroluminescent refrigeration regime [13]. The cooling power of an OLED is therefore also reduced relative to an inorganic LED operating at the same voltage, with all other factors being equal.

The energetic disorder characteristic of most OLED devices can be accounted for using the same framework. In the commonly-assumed case of a Gaussian density of states (DOS) [10] for electrons, holes, and excitons (with respective variances σ_n^2 , σ_p^2 , and σ_x^2), the Supplemental Material [22] shows that the overpotential is still given by Eq. (6), but with an effective exciton binding energy given by $E'_b = E_b + (\sigma_x^2 - \sigma_n^2 - \sigma_p^2)/(2k_B T)$. Figure 3(a) compares the absorption and emission spectra of an ideal sharp exciton band to one with a Gaussian line shape having the same optical gap (defined as two standard deviations below the mean). The Stokes shift between absorption and emission in the latter case is approximately $\sigma_{\text{abs}}^2/k_B T$; in the following we assume the variance of the absorption band (σ_{abs}^2) is equal to that of the exciton DOS for simplicity (i.e., homogeneous broadening is negligible).

Figure 3(b) shows the voltage required for the sharp gap and disordered OLEDs to emit an intensity of $1 \mu\text{W cm}^{-2}$ (close to 1 cd m^{-2} for a typical green OLED) as a function of average emitted photon energy. It is evident that there is little difference between the sharp gap and disordered thermodynamic limits, and that the best OLEDs reported to date are within a few tenths of a volt of the limit, depending on their exciton binding energy. Given the likelihood that E_b for phosphorescent and TADF emitters lies between 0.5 and 1 eV, [36,37] one might conclude that several of these devices do in fact operate at their thermodynamic limit, validating the assertion made in Ref. [2].

To eliminate the overpotential and reach the inorganic LED limit, exciton dissociation must be efficient. This may seem counterintuitive since exciton dissociation has often been viewed as a loss mechanism in OLEDs; however, provided that all charge carriers eventually recombine (and non-idealities such as exciton-polaron quenching are negligible), there is in fact no efficiency loss. Resonant injection into, e.g., the triplet state of a phosphor [38,39] as illustrated in Fig. 4, is one example that nominally satisfies the dissociation criterion since, if injection into the exciton state is resonant, so is dissociation. Donor-acceptor type exciplex-charge transfer (CT) state emissive layers that exhibit efficient emission and photocurrent generation [40,41] are another example (see Fig. 4). These systems possess both a low CT state binding energy and a relatively low radiative rate ($\sim 1 \mu\text{s}^{-1}$ owing to the spatially indirect nature of the transition, which also affords efficient singlet-triplet spin mixing) that make them suited to reach the inorganic LED limit. Note that this excludes donor-acceptor OLEDs that produce electroluminescence at “half-gap” voltages via up-conversion [42,43] since

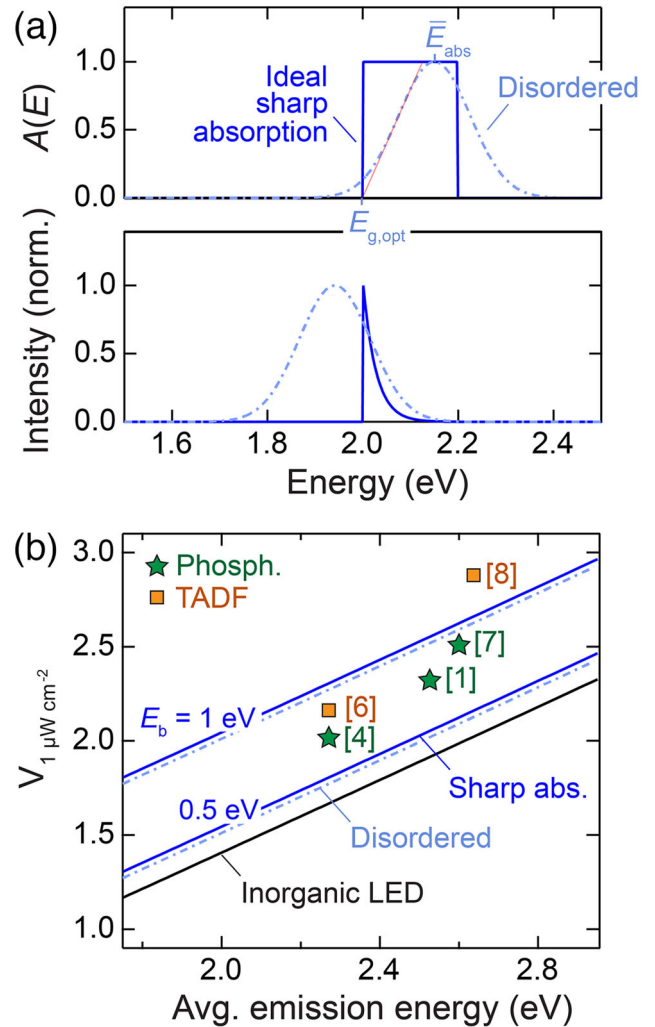


FIG. 3. (a) Absorbance (top) and emission (bottom) spectra for an OLED with an idealized sharp excitonic absorption band and one with a Gaussian line shape with a mean energy, \bar{E}_{abs} , and standard deviation σ_{abs} . The optical gap of the latter is defined by the x -intercept of the tangent to the inflection point of the Gaussian, $E_{g,\text{opt}} = \bar{E}_{\text{abs}} - 2\sigma_{\text{abs}}$. Note that the Gaussian absorbance continues well below $E_{g,\text{opt}}$ and is responsible for the emission at lower photon energies. (b) Voltage required to produce an output intensity of $1 \mu\text{W cm}^{-2}$ as a function of the average emission energy for each device assuming the same parameters as in Fig. 2(b), with $\sigma_{\text{abs}} = \sigma_x = \sigma_n = \sigma_p = 75 \text{ meV}$ for the disordered case (dash-dotted lines). Symbols (with associated references in parentheses) indicate the lowest experimental operating voltages that have been reported at this output intensity for OLEDs with phosphorescent and TADF emissive layers.

they inherently operate below the thermodynamic limit (i.e., not all recombination is radiative). In principle, the *intramolecular* charge separation characteristic of TADF emitters [44] is expected to reduce their exciton binding energy [45] and thereby facilitate a smaller thermodynamic overpotential than a comparable phosphorescent emitter in

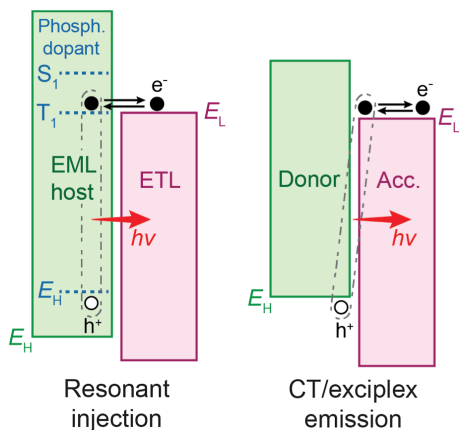


FIG. 4. Energy level diagram illustrating resonant injection and extraction from the triplet exciton state (T_1) of a phosphorescent emitter (left-hand diagram) and the charge transfer state of a donor-acceptor emissive layer (right-hand diagram).

the absence of resonant injection, though such an effect is not observed in the experimental data of Fig. 3(b).

Finally, although long exciton lifetime is beneficial for reducing the thermodynamic overpotential of an ideal OLED, it is generally detrimental for practical devices because it exacerbates (nonideal) bimolecular annihilation processes that reduce device efficiency and lifetime [46]. At least for display and lighting applications, it is therefore preferable to minimize ΔV_{op} by reducing E_b and increasing charge carrier mobility rather than deliberately attempting to increase the exciton lifetime.

In summary, we have shown that strong exciton binding in OLEDs necessitates higher voltage to achieve a given luminance in the thermodynamic limit than for the case of inorganic LEDs where free carriers are the primary optical excitation. In addition to a small exciton binding energy, the OLED overpotential is minimized by having a small radiative decay rate and a high Langevin recombination coefficient. Based on these results, it seems likely that the best phosphorescent and TADF OLEDs to date have reached their thermodynamic limit. The framework developed here is general, and can be applied to LEDs based on other excitonic materials such as colloidal quantum dots, halide perovskites, and two-dimensional semiconductors, provided that their equilibrium relation between excitons and free carriers (e.g., the Saha-Langmuir equation for Wannier excitons [17,47,48]) is known. These results should therefore help benchmark and guide the development of low voltage excitonic LEDs for the next generation of displays and solid-state lighting.

N. C. G. was supported by the U.S. Department of Energy EERE SSL program under Award No. DE-EE0009694. S. R. F. acknowledges support for the National Science Foundation, Grant No. DMR-1905401, and Universal Display Corp. (UDC). One of the authors (S. R. F.) has an equity interest in one of the sponsors of this work

(UDC). This conflict is under management by the University of Michigan Office of the Vice President for Research. The University of Michigan has a royalty bearing license with UDC.

*ngiebink@umich.edu

- [1] K. Udagawa, H. Sasabe, C. Cai, and J. Kido, Low-driving-voltage blue phosphorescent organic light-emitting devices with external quantum efficiency of 30%, *Adv. Mater.* **26**, 5062 (2014).
- [2] R. Meerheim, K. Walzer, G. He, M. Pfeiffer, and K. Leo, Highly efficient organic light emitting diodes (OLED) for displays and lighting, in *Organic Optoelectronics and Photonics II*, edited by P. L. Heremans, M. Muccini, and E. A. Meulenkaamp (SPIE, 2006), 6192, 61920P.
- [3] G. He, O. Schneider, D. Qin, X. Zhou, M. Pfeiffer, and K. Leo, Very high-efficiency and low voltage phosphorescent organic light-emitting diodes based on a p-i-n junction, *J. Appl. Phys.* **95**, 5773 (2004).
- [4] H. Sasabe, H. Nakanishi, Y. Watanabe, S. Yano, M. Hirasawa, Y.-J. Pu, and J. Kido, Extremely low operating voltage green phosphorescent organic light-emitting devices, *Adv. Funct. Mater.* **23**, 5550 (2013).
- [5] S.-J. Su, H. Sasabe, Y.-J. Pu, K. Nakayama, and J. Kido, Tuning energy levels of electron-transport materials by nitrogen orientation for electrophosphorescent devices with an 'Ideal' operating voltage, *Adv. Mater.* **22**, 3311 (2010).
- [6] H. Sasabe, R. Sato, K. Suzuki, Y. Watanabe, C. Adachi, H. Kaji, and J. Kido, Ultrahigh power efficiency thermally activated delayed fluorescent OLEDs by the strategic use of electron-transport materials, *Adv. Opt. Mater.* **6**, 1800376 (2018).
- [7] J. Jia, L. Zhu, Y. Wei, Z. Wu, H. Xu, D. Ding, R. Chen, D. Ma, and W. Huang, Triazine-phosphine oxide electron transporter for ultralow-voltage-driven sky blue PHOLEDs, *J. Mater. Chem. C* **3**, 4890 (2015).
- [8] D. Zhang, M. Cai, Z. Bin, Y. Zhang, D. Zhang, and L. Duan, Highly efficient blue thermally activated delayed fluorescent OLEDs with record-low driving voltages utilizing high triplet energy hosts with small singlet-triplet splitting, *Chem. Sci.* **7**, 3355 (2016).
- [9] P. Würfel, The chemical potential of radiation, *J. Phys. C* **15**, 3967 (1982).
- [10] S. R. Forrest, *Organic Electronics: Foundations to Applications* (Oxford University Press, New York, 2020).
- [11] N. C. Giebink, G. P. Wiederrecht, M. R. Wasielewski, and S. R. Forrest, Thermodynamic efficiency limit of excitonic solar cells, *Phys. Rev. B* **83**, 195326 (2011).
- [12] R. A. J. Janssen and J. Nelson, Factors limiting device efficiency in organic photovoltaics, *Adv. Mater.* **25**, 1847 (2013).
- [13] T. Patrick Xiao, K. Chen, P. Santhanam, S. Fan, and E. Yablonovitch, Electroluminescent refrigeration by ultra-efficient GaAs light-emitting diodes, *J. Appl. Phys.* **123**, 173104 (2018).
- [14] E. H. Kennard, On the thermodynamics of fluorescence, *Phys. Rev.* **11**, 29 (1918).

- [15] B. I. Stepanov, A universal relation between the absorption and luminescence spectra of complex molecules, *Sov. Phys. Dokl.* **2**, 81 (1957).
- [16] R. L. van Metter and R. S. Knox, On the relation between absorption and emission spectra of molecules in solution, *Chem. Phys.* **12**, 333 (1976).
- [17] C. L. Braun, Electric field assisted dissociation of charge transfer states as a mechanism of photocarrier production, *J. Chem. Phys.* **80**, 4157 (1984).
- [18] I. Amdur and G. Hammes, *Chemical Kinetics: Principles and Selected Topics* (McGraw-Hill, New York, 1966).
- [19] M. Wojcik and M. Tachiya, Accuracies of the empirical theories of the escape probability based on Eigen model and Braun model compared with the exact extension of Onsager theory, *J. Chem. Phys.* **130**, 104107 (2009).
- [20] V. D. Mihailetschi, L. J. A. Koster, J. C. Hummelen, and P. W. M. Blom, Photocurrent Generation in Polymer-Fullerene Bulk Heterojunctions, *Phys. Rev. Lett.* **93**, 216601 (2004).
- [21] T. M. Clarke and J. R. Durrant, Charge photogeneration in organic solar cells, *Chem. Rev.* **110**, 6736 (2010).
- [22] See Supplemental Material at <http://link.aps.org/supplemental/10.1103/PhysRevLett.130.267002> for a derivation of the current-voltage relationship for an ideal OLED, numerical drift-diffusion modeling, extension of the thermodynamic limit framework to include energetic disorder, and analytical expressions for the luminescent photon flux in Eq. (1), which includes Refs. [23–34].
- [23] Y. Li, O. Sachnik, B. Zee, K. Thakur, C. Ramanan, G.-J. A. H. Wetzelaer, and P. W. M. Blom, Universal electroluminescence at voltages below the energy gap in organic light-emitting diodes, *Adv. Opt. Mater.* **9**, 2101149 (2021).
- [24] N. C. Giebink, G. P. Wiederrecht, M. R. Wasielewski, and S. R. Forrest, Ideal diode equation for organic heterojunctions. I. Derivation and application, *Phys. Rev. B* **82**, 155305 (2010).
- [25] T. Trupke, M. A. Green, P. Würfel, P. P. Altermatt, A. Wang, J. Zhao, and R. Corkish, Temperature dependence of the radiative recombination coefficient of intrinsic crystalline silicon, *J. Appl. Phys.* **94**, 4930 (2003).
- [26] J. G. Simmons and G. W. Taylor, Nonequilibrium steady-state statistics and associated effects for insulators and semiconductors containing an arbitrary distribution of traps, *Phys. Rev. B* **4**, 502 (1971).
- [27] B. E. Pieters, T. Kirchartz, T. Merdzhanova, and R. Carius, Modeling of photoluminescence spectra and quasi-Fermi level splitting in $\mu\text{-Si:H}$ solar cells, *Sol. Energy Mater. Sol. Cells* **94**, 1851 (2010).
- [28] J. J. M. Van Der Holst, F. W. A. Van Oost, R. Coehoorn, and P. A. Bobbert, Electron-hole recombination in disordered organic semiconductors: Validity of the Langevin formula, *Phys. Rev. B* **80**, 235202 (2009).
- [29] A. Massé, P. Friederich, F. Symalla, F. Liu, V. Meded, R. Coehoorn, W. Wenzel, and P. A. Bobbert, Effects of energy correlations and superexchange on charge transport and exciton formation in amorphous molecular semiconductors: An *ab initio* study, *Phys. Rev. B* **95**, 115204 (2017).
- [30] G. G. Malliaras and J. C. Scott, Numerical simulations of the electrical characteristics and the efficiencies of single-layer organic light emitting diodes, *J. Appl. Phys.* **85**, 7426 (1999).
- [31] W. Brütting, S. Berleb, and A. G. Mückl, Device physics of organic light-emitting diodes based on molecular materials, *Org. Electron.* **2**, 1 (2001).
- [32] R. Coehoorn and S. L. M. Van Mensfoort, Effects of disorder on the current density and recombination profile in organic light-emitting diodes, *Phys. Rev. B* **80**, 085302 (2009).
- [33] L. J. A. Koster, E. C. P. Smits, V. D. Mihailetschi, and P. W. M. Blom, Device model for the operation of polymer/fullerene bulk heterojunction solar cells, *Phys. Rev. B* **72**, 085205 (2005).
- [34] G. A. H. Wetzelaer, M. Kuik, H. T. Nicolai, and P. W. M. Blom, Trap-assisted and Langevin-type recombination in organic light-emitting diodes, *Phys. Rev. B* **83**, 165204 (2011).
- [35] T. M. Burke, S. Sweetnam, K. Vandewal, and M. D. McGehee, Beyond Langevin recombination: How equilibrium between free carriers and charge transfer states determines the open-circuit voltage of organic solar cells, *Adv. Energy Mater.* **5**, 1500123 (2015).
- [36] M. Knupfer, Exciton binding energies in organic semiconductors, *Appl. Phys. A* **77**, 623 (2003).
- [37] H. Yoshida and K. Yoshizaki, Electron affinities of organic materials used for organic light-emitting diodes: A low-energy inverse photoemission study, *Org. Electron.* **20**, 24 (2015).
- [38] R. J. Holmes, B. W. D'Andrade, S. R. Forrest, X. Ren, J. Li, and M. E. Thompson, Efficient, deep-blue organic electrophosphorescence by guest charge trapping, *Appl. Phys. Lett.* **83**, 3818 (2003).
- [39] S. R. Forrest, J. J. Brown, and M. E. Thompson, OLEDs utilizing direct injection to the triplet state, US Patent No. 7683536B2 (2010).
- [40] S. Ullbrich *et al.*, Emissive and charge-generating donor-acceptor interfaces for organic optoelectronics with low voltage losses, *Nat. Mater.* **18**, 459 (2019).
- [41] B. Liang, J. Wang, Z. Cheng, J. Wei, and Y. Wang, Exciplex-based electroluminescence: Over 21% external quantum efficiency and approaching 100 lm/W power efficiency, *J. Phys. Chem. Lett.* **10**, 2811 (2019).
- [42] A. K. Pandey and J. M. Nunzi, Upconversion injection in rubrene/perylene-diimide-heterostructure electroluminescent diodes, *Appl. Phys. Lett.* **90**, 263508 (2007).
- [43] C. Xiang, C. Peng, Y. Chen, and F. So, Origin of sub-bandgap electroluminescence in organic light-emitting diodes, *Small* **11**, 5439 (2015).
- [44] H. Nakanotani, Y. Tsuchiya, and C. Adachi, Thermally-activated delayed fluorescence for light-emitting devices, *Chem. Lett.* **50**, 938 (2021).
- [45] X. Liu, Y. Li, K. Ding, and S. Forrest, Energy Loss in Organic Photovoltaics: Nonfullerene Versus Fullerene Acceptors, *Phys. Rev. Appl.* **11**, 024060 (2019).
- [46] N. C. Giebink, B. W. D'Andrade, M. S. Weaver, P. B. Mackenzie, J. J. Brown, M. E. Thompson, and S. R. Forrest, Intrinsic luminance loss in phosphorescent small-molecule organic light emitting devices due to

- bimolecular annihilation reactions, *J. Appl. Phys.* **103**, 044509 (2008).
- [47] V. D’Innocenzo, G. Grancini, M.J.P. Alcocer, A.R.S. Kandada, S.D. Stranks, M.M. Lee, G. Lanzani, H.J. Snaith, and A. Petrozza, Excitons versus free charges in organo-lead tri-halide perovskites, *Nat. Commun.* **5**, 3586 (2014).
- [48] A. A. Lipnik, Binding and decay of the mott exciton by phonons and impurity centers, *Sov. Phys. Solid State* **3**, 1683 (1962).